

# Magnetoresistance in ordered and disordered double perovskite oxide, $\text{Sr}_2\text{FeMoO}_6$

D. D. Sarma<sup>a</sup>, E.V. Sampathkumaran<sup>b</sup>, Sugata Ray<sup>a</sup>, R. Nagarajan<sup>b</sup>, Subham Majumdar<sup>b</sup>,  
Ashwani Kumar<sup>a</sup>, G. Nalini<sup>a</sup> and T.N. Guru Row<sup>a</sup>

<sup>a</sup>*Solid State and Structural Chemistry Unit, Indian Institute of Science, Bangalore 560 012, India*

<sup>b</sup>*Tata Institute of Fundamental Research, Mumbai - 400 005, India*

(February 1, 2008)

## Abstract

We have prepared crystallographically ordered and disorder specimens of the double perovskite,  $\text{Sr}_2\text{FeMoO}_6$  and investigated their magnetoresistance behaviour. The extent of ordering between the Fe and Mo sites in the two samples is determined by Rietveld analysis of powder x-ray diffraction patterns and reconfirmed by Mössbauer studies. While the ordered sample exhibits the sharp low-field response, followed by moderate changes in the magnetoresistance at higher fields, the disordered sample is characterised by the absence of the spectacular low-field response. We argue that the low field response depends crucially on the half-metallic ferromagnetism, while the high-field response follows from the overall magnetic nature of the sample, even in absence of the half-metallic state.

**Keywords:** A. magnetically ordered materials, D. electronic transport, order-disorder effects, E. x-ray and  $\gamma$ -ray spectroscopies.

## I. INTRODUCTION

Colossal magnetoresistance (CMR) is a property that is of great technological potential, since the large change in the resistance ( $R$ ) with the application of a magnetic field can be used effectively for mass storage magnetic devices. However, the well-known CMR materials, Mn based oxides, have significant CMR effect only at low temperatures and, therefore, are not suitable for room temperature applications. In their recent work, Kobayashi *et al.* [1] have pointed out that the fully-ordered double perovskite  $\text{Sr}_2\text{FeMoO}_6$  with alternating  $\text{Fe}^{3+}$  ( $3d^5$ ,  $S = 5/2$ ) and  $\text{Mo}^{5+}$  ( $4d^1$ ,  $S = 1/2$ ) ferrimagnetically coupled ions exhibit substantial CMR even at room temperature. It is suggested that the half-metallic ferromagnetic (HMFM) state below  $T_c$  is responsible for the magnetoresistance (MR) behavior via spin-dependent carrier scattering processes. While the spin-dependent scattering due to the intergrain tunneling effects enables one to construct manganite based devices [2], the intra-grain properties of the manganites are generally believed to be intimately connected with the intrinsic instability of  $\text{Mn}^{3+}$   $3d^4$  states arising from strong electron-phonon interaction as well as double-exchange interaction [3,4].  $\text{Mo}^{5+}$  is also a Jahn-Teller ion with its  $4d^1$   ${}^2D$  degenerate ground state. Thus, *a priori* it is not possible to rule out any contribution to the magnetoresistance of  $\text{Sr}_2\text{FeMoO}_6$  from effects other than intergrain spin-dependent carrier scatterings. Considering the complexity of the mechanism of magnetoresistance in the manganites, in which in addition to half-metallic ferromagnetism, various instabilities play important role, it is essential to address the factors responsible for the novel magnetoresistance properties of  $\text{Sr}_2\text{FeMoO}_6$ .

Central to the HMFM state in  $\text{Sr}_2\text{FeMoO}_6$  as deduced by the band structure calculation [1] is the long-range ordering of  $\text{FeO}_6$  and  $\text{MoO}_6$  octahedra alternately along three cubic axes. Disorder is expected to be detrimental to the half-metallic nature, giving rise to finite up- and down-spin densities of states at the Fermi energy, destroying the HMFM state; preliminary super-cell band structure calculations in our group indeed suggest that HMFM state is easily destroyed by a positional disorder at the Fe/Mo sites, though an over-

all ferrimagnetic order persists in the system. Keeping this in mind we have prepared for the first time  $\text{Sr}_2\text{FeMoO}_6$  by melt-quenching, where Fe and Mo sites are heavily disordered. A comparative study of disordered and ordered samples using x-ray diffraction,  $^{57}\text{Fe}$  Mössbauer and the magnetoresistive properties allows us to delineate the effects arising from long range crystallographic order and those from factors other than half-metallic ferromagnetism in controlling the MR properties.

## II. EXPERIMENTAL

We prepared ordered  $\text{Sr}_2\text{FeMoO}_6$  following ref. 1 by hydrogen reduction of a mixture of  $\text{SrCO}_3$ ,  $\text{MoO}_3$  and  $\text{Fe}_2\text{O}_3$ . The disordered sample was prepared by melt-quenching of a mixture of  $\text{SrCO}_3$ ,  $\text{MoO}_3$ ,  $\text{Fe}_2\text{O}_3$  and Mo-metal in an argon atmosphere. Mössbauer study was carried out in transmission geometry using a  $^{57}\text{Co}/\text{Rh}$  matrix source. High resolution powder diffraction data were collected on a STOE STADI/P diffractometer. The resistivity measurements with and without an applied field were carried out using the standard four-probe dc measurements.

## III. RESULTS AND DISCUSSION

We show the powder x-ray diffraction patterns of the two samples in Fig. 1; Fig. 1(a) shows the pattern of the sample prepared by the conventional solid state techniques [1], while Fig. 1(b) shows the same for the melt-quenched sample prepared by the arc melting. The main diffraction peaks are the same in both the panels of Fig. 1 and these are readily ascribed to the perovskite lattice. The only difference between the two diffraction patterns is in terms of the existence of two weak peaks, at  $19.6^\circ$  and  $38^\circ$  in Fig. 1(a), but absence in Fig. 1(b). We have expanded the vicinity of these two angles in order to illustrate this point clearly in the respective panels. The existence of these two peaks in Fig. 1(a) establishes the presence of the supercell arising from the ordering of Fe and Mo sites alternately, giving rise to the double perovskite structure. Total or near-absence of these two order-related

peaks in Fig. 1(b) suggests that the melt-quenched sample obtained from the arc furnace gives rise to heavy disordering between the Fe and the Mo sites. The extent of ordering at the Fe/Mo sites is easily estimated from x-ray diffraction (XRD) of ordered (**A**) [Fig. 1(a)] and disordered (**B**) [Fig. 1(b)] samples of  $\text{Sr}_2\text{FeMoO}_6$ . Rietveld refinement for both converged to the same cell dimensions ( $a = b = 5.566 \text{ \AA}$  and  $c = 7.858 \text{ \AA}$ ) with  $R_{wp} \leq 8.0\%$ . The ordering at the Fe and Mo sites in sample **A** was found to be  $\sim 91\%$ , slightly larger than the previously reported [1] value of 87%. Near-absence of the long-range order-related peaks within the noise level of the data [see insets I and II to Fig. 1(b)] for sample **B** confirms the extensive disorder in this case. Rietveld analysis suggests approximately 31% ordering in this case.

The effect of disorder at the Fe-sites is also probed by  $^{57}\text{Fe}$  Mössbauer spectra of these two samples at 300 K and 4.2 K (Fig. 2); a comparison of the raw spectra for the two samples at these temperatures is sufficient to establish the relative degrees of disorder in site occupancies. The spectra for the sample **B** exhibits relatively larger line-widths in contrast to those of sample **A**, implying a larger disorder in sample **B**. All the spectra are magnetic hyperfine split, indicating magnetic ordering of the materials. The spectrum at 300 K for sample **A** favorably compares with that reported earlier [5]. Our analysis of the data at 4.2 K for sample **A** yields a saturation hyperfine field of about 480 kOe, with a small distribution of about 10 kOe. This value is somewhat smaller than that known for  $\text{Fe}_2\text{O}_3$ . The hyperfine field for sample **B** has a much larger distribution ( $490 \pm 60 \text{ kOe}$ ), quantitatively confirming a strong variation in the chemical environment for Fe from site to site. The chemical composition was however found to be identical between the two samples by energy dispersive x-ray analysis. Moreover, the grain size and morphology were also found to be similar between the two samples by scanning electron microscopy (SEM). The above results establish that it is indeed possible to obtain highly ordered and extensively disordered samples with respect to Fe and Mo occupancies without otherwise disturbing the structural integrity of this double perovskite system.

We show the magnetoresistance,  $MR(H, T) = \{R(H, T) - R(0, T)\}/R(0, T)$ , of ordered

and disordered samples as a function of applied magnetic field,  $H$ , at 300 K and 4.2 K in Fig 3; in the same figure we reproduce the results from Kobayashi *et al.* [1]. At both the temperatures, the ordered sample is characterised by a sharp magnetoresistive response in the low-field region, though the magnitude of the magnetoresistance is considerably larger at the lower temperature, in agreement with the published literature [1]. The present ordered sample has a sharper low-field response and a larger magnitude, particularly at the low temperature compared to the previous result [1]. This improved magnetoresistance response is possibly related to somewhat higher degree of ordering in the present sample. This improvement in the low magnetic field response suggests that a fully (100%) ordered sample is likely to be a very good candidate for real-life device applications. Beyond about 1 T, the magnetoresistance of the ordered sample exhibits a slower change at higher field strengths, without showing any signs of saturation upto the highest magnetic field probed in the present experiments. The MR changes significantly (by about 6.5% at 4.2 K and 3% at 300 K) in the larger field regime between 1 and 7 T.

In contrast, the MR of the disordered sample does not exhibit the low-field sharp magnetic response below 1 T. Since the two samples differ only in the extent of Fe/Mo ordering, the low-field rapid variation in MR of sample **A** evidently arises from the long-range order, leading to the half metallic ferromagnetic state of sample **A** and the consequent strong intergrain spin-dependent scattering. It is, however, intriguing to note that there is a substantial negative magnetoresistance in the disordered sample and the high field behaviors of the MR in the two samples are similar, the two curves being approximately parallel in the high-field region at both the temperatures shown in Fig. 3. This implies that there is a common intragrain origin of this high-field MR behavior in the disordered and the ordered samples.

We have carried out band structure calculations, simulating the disordered system within a supercell approach where the Fe and Mo atoms were allowed to occupy the other sites in contrast to the perfectly ordered system. Preliminary results from these calculations show that in the disordered state, both up- and down-spin states exist at the Fermi energy; this

indicates that the half-metallic ferromagnetic ground state is not realised for any disordering of the Fe and the Mo sublattices, though the system remains to be a ferrimagnet. Thus, the high-field, intragrain contribution to the negative magnetoresistance is independent of the long range ordering of Fe and Mo atoms and the consequent existence of the HMF state. Instead, it is to be associated with the usual negative magnetoresistance observed for ferromagnetic substances, arising from a suppression of the spin-fluctuations with the application of an external magnetic field.

In conclusion, we have prepared highly ordered and disordered samples of the perovskite oxide,  $\text{Sr}_2\text{FeMoO}_6$ . We characterised the extent of ordering by x-ray diffraction and Mössbauer studies of these samples. Rietveld analysis of the powder diffraction pattern shows that the extent of ordering in the Fe/Mo sites is about 91% for the ordered sample, while it is about 31% for the disordered sample. We point out that the disordered sample is not a half-metallic ferromagnet, though it is magnetic even at the room temperature. We showed that the magnetoresistance of the two samples are distinguished by the existence of the sharp changes in the magnetoresistance at low fields for the ordered sample. In the case of the disordered sample, there is no such sharp changes in the MR, though a negative MR is seen at all fields for the disordered sample also. The MR of the disordered sample is very similar to that of the ordered sample in the high-field regime, indicating a common origin. Thus, we conclude that the low-field magnetoresistance is dominated by the intergrain spin-dependent scattering of the highly spin polarized charge-carriers of the half-metallic ferromagnet, the high-field negative magnetoresistance behaviours in both the samples are intrinsic, intragrain property and arise from the suppression of spin-fluctuations under the application of a magnetic field on a magnetic system.

**Acknowledgements:** The authors thank Prof. B. Sriram Shastry and Dr. Tanusri Saha Dasgupta for useful discussions.

## REFERENCES

- [1] K. -I. Kobayashi, T. Kimura, H. Sawada, K. Terakura and Y. Tokura, *Nature* 395 (1998) 677.
- [2] N.D. Mathur, Burnell G., Isaac S.P., Jackson T.J., Teo B.S., MacManusDriscoll J.L., Cohen L.F., Evetts J.E., Blamire M.G., *Nature* 387 (1997) 266.
- [3] A.J. Millis, P. B. Littlewood and B. I. Shraiman, *Phys. Rev. Lett.* 74 (1995) 5144.
- [4] A.J. Millis, B. I. Shraiman and R. Mueller, *Phys. Rev. Lett.* 77 (1996) 175.
- [5] T. Nakagawa, *J. Phys. Soc. Japan* 24 (1968) 806.

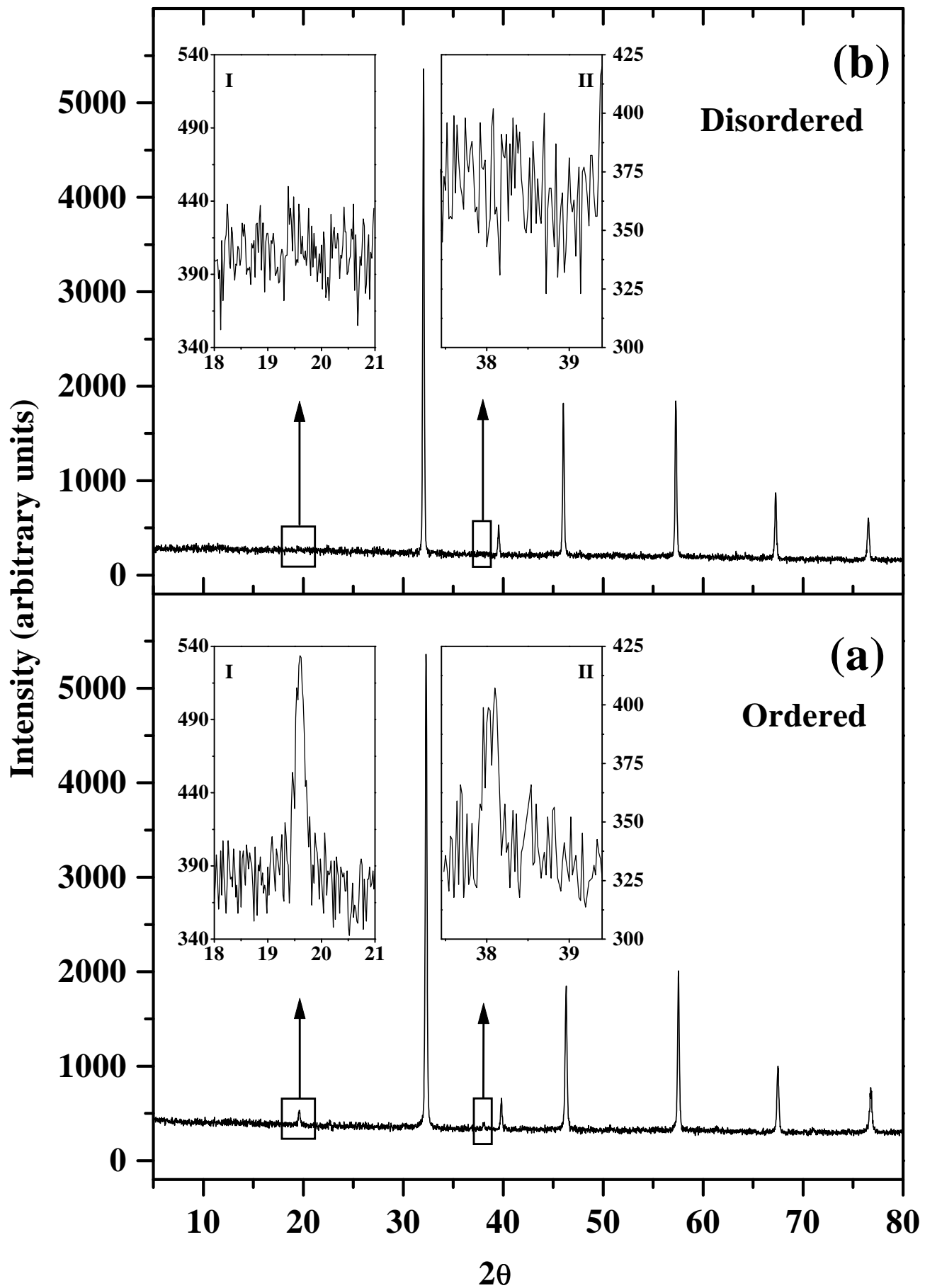
#### IV. FIGURE CAPTIONS

Fig. 1. X-ray diffraction patterns of (a) ordered and (b) disordered  $\text{Sr}_2\text{FeMoO}_6$ . Order-related peaks, appear at  $19.6^\circ$  and  $38^\circ$ , shown in the insets on an expanded scale.

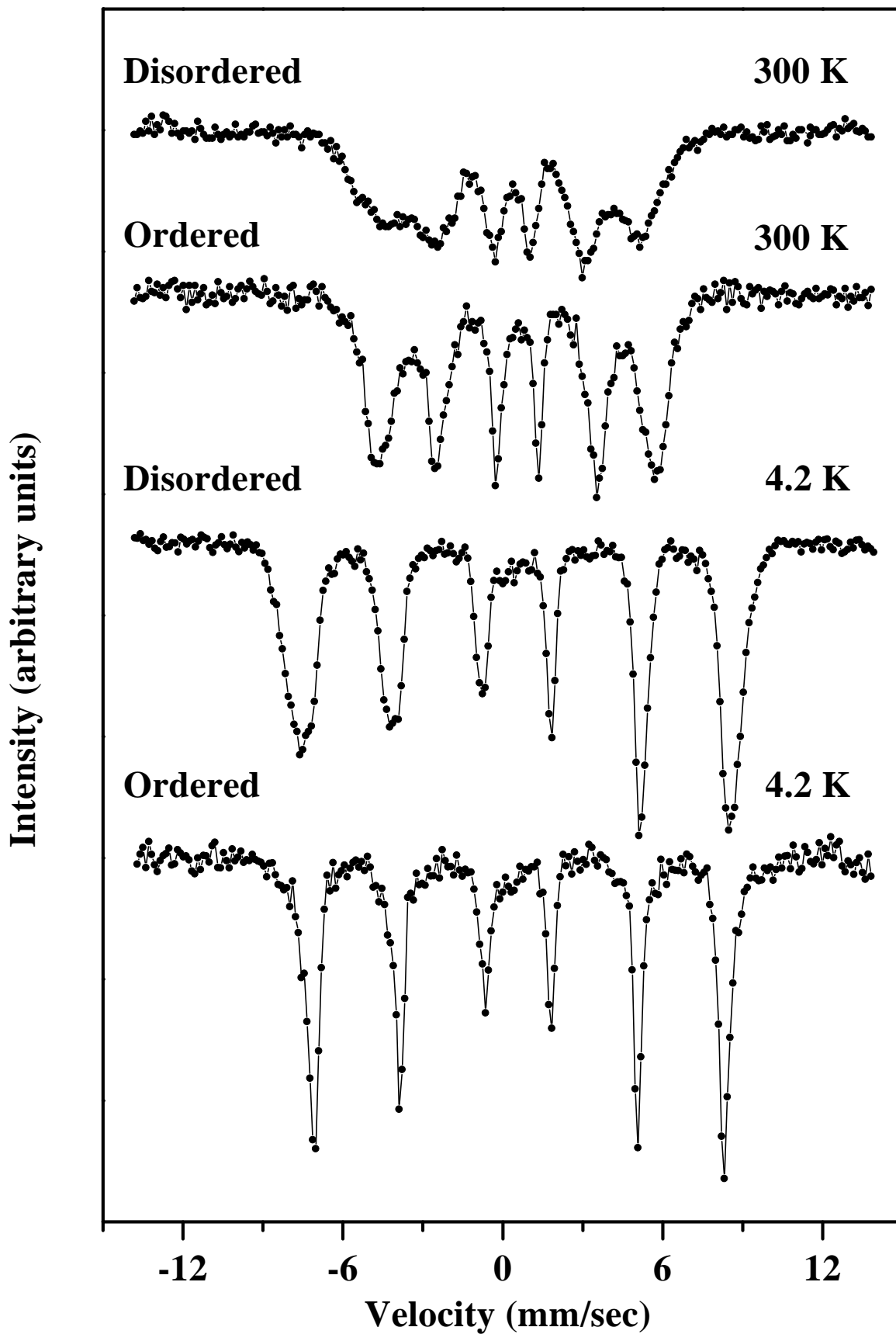
Fig. 2.  $^{57}\text{Fe}$  Mössbauer spectra of the disordered and ordered  $\text{Sr}_2\text{FeMoO}_6$  at 300 and 4.2 K.

Fig. 3. The comparisons of percentage magnetoresistance between the ordered and disordered samples as well as the result presented by Kobayashi *et al.* [1] at (a) 4.2 K and (b) 300 K.

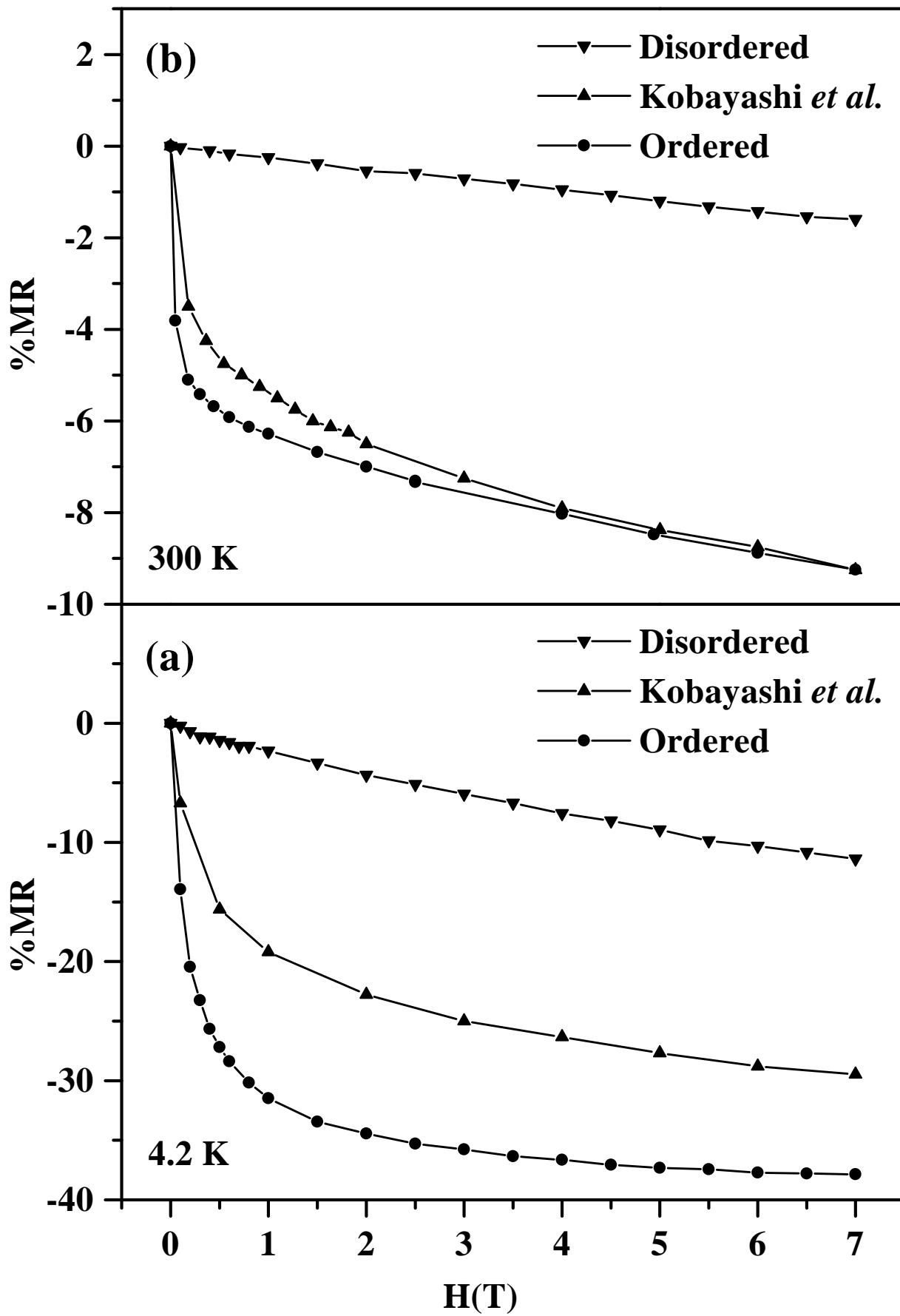




Sarma *et al.*, Fig. 1



Sarma *et al.*, Fig. 2



Sarma *et al.*, Fig. 3